www.sciencetranslationalmedicine.org/cgi/content/full/6/241/241ra79/DC1

Supplementary Materials for

Selective Targeting of TGF-β Activation to Treat Fibroinflammatory Airway Disease

Shunsuke Minagawa, Jianlong Lou, Robert I. Seed, Anthony Cormier, Shenping Wu, Yifan Cheng, Lynne Murray, Ping Tsui, Jane Connor, Ronald Herbst, Cedric Govaerts, Tyren Barker, Stephanie Cambier, Haruhiko Yanagisawa, Amanda Goodsell, Mitsuo Hashimoto, Oliver J. Brand, Ran Cheng, Royce Ma, Kate J. McKnelly, Weihua Wen, Arthur Hill, David Jablons, Paul Wolters, Hideya Kitamura, Jun Araya, Andrea J. Barczak, David J. Erle, Louis F. Reichardt, James D. Marks, Jody L. Baron, Stephen L. Nishimura*

*Corresponding author. E-mail: stephen.nishimura@ucsf.edu

Published 18 June 2014, *Sci. Transl. Med.* **6**, 241ra79 (2014)
DOI: 10.1126/scitranslmed.3008074

The PDF file includes:

Supplementary Materials

Materials and Methods:

Cells and reagents: Adult lung parenchyma was collected from lobectomy specimens from resections performed for primary lung cancer or from normal lungs not used for transplantation. Lung tissue was considered "normal" if the pulmonary function was normal. Fetal organs and tracheas were obtained at the time of elective termination of pregnancy (18 to 21 weeks gestation) from otherwise healthy females. Informed consent was obtained from all study participants as part of an approved ongoing research protocol by the University of California San Francisco Committee on Human Research in full accordance with the declaration of Helsinki principles. Tracheal and lung fibroblasts were cultured by the explant technique and used P1 to P4 (*52*). Cell culture media and antibiotics were prepared by the University of California, San Francisco Cell Culture Facility using deionized water and analytical grade reagents. Fetal calf serum was obtained from Invitrogen (Carlsbad, CA), human recombinant IL-1β and TGF-β1 were obtained from R&D Systems (Minneapolis, MN). Human embryonic kidney 293 cells, HT1080 and Hybridoma clone 1D11 were obtained from the American Tissue Type Collection (ATCC, Manassus, VA). P3U1 cells over-expressing murine TGF-β1 have been described (*53*) and were a gift of Howard Weiner (Harvard Medical School, Boston, MA). Clone 1D11 is a pan-TGF-β isoform monoclonal antibody which cross reacts with TGF-β1, 2, 3 of human, mink and mouse origin. Anti-SV5 (*54*) and anti-human MHC class I (clone W6/32 IgG2a, ATCC) hybridomas were grown and purified using FPLC, as previously described (*55*). Antibodies were tested for endotoxin to confirm endotoxin levels <0.2 EU/μg as determined by LAL method, (Genscript, Piscataway, NJ). ELISA kits human CCL2 (Cat#DY279), human CCL20 (Cat#DY360), mouse CCL2 (Cat#DY479), mouse CCL20 (Cat#DY760), mouse IL-17 (Cat#M1700), mouse IL-1α (Cat#MLA00), mouse IL-1β (Cat#MLB00B) and mouse myeloperoxidase (Cat#DY3667) were from R&D systems and pSMAD2 ELISA (#7348) from Cell Signaling Technology (Danvers, MA). Rabbit monoclonal anti-mouse pSMAD3 (EP823Y) was from Epitomics (Burlingame, CA). TMLC TGF-β reporter cells were maintained in 10% FCS in DMEM (gift of John Munger, New York University Medical Center, NYC, NY). Simian LAP (a gift from John Munger, NYU, NYC, NY) was prepared from baculovirus, as described (*56*).

BAC copy number determination: The size of the mouse genome based on the average genome size of five assemblies (GRCm38.p1, Mm_Celera, GRCm38.p2, MmusSOAP1 & mm129svJae1.0) was estimated to be 2,785.85Mb. We calculated the copy number of a given template using web-based tools (http://www.uri.edu/research/gsc/resources/cndna.html). Based on this genome size, 20ng of mouse genomic DNA contains approximately 6,650 haploid genome copies. To generate a standard curve we used 20 ng of wild-type mouse gDNA spiked with 2 μl of a plasmid diluted with a known copy number containing the targeted region to generate curve standards. Primers used were 5'-TGCCCGCCACAAATCTG-3' and 5'-ATCGAAGGTTTGCAACTTCCA-3' for gene copy determination. Copy number was determined using qPCR of tail-tip DNA. BAC copy number analysis revealed that lines B and C express 2 copies and line D express 1 copy of the *ITGB8* BAC. Mouse and human organ ELISA assays were performed to assess the organ distribution of human β8 from 100 μg of organ lysates. ELISA for αvβ8 protein revealed a gene dose-dependent increase in αvβ8 protein in organs where β8 was expressed (**Fig. *S1***). We used human fetal tissue as control samples to show that the general organ distribution remained the same between the transgenic mice and human fetus (**Fig. *S1***). All three lines of mice completely rescued the lethality and pathology of deficiency of germline deletion of mouse *itgb8* in the first 6 months indicating that RP11-431K20 contains the key regulatory regions required for developmental (vasculogenesis and brain) and homeostatic (DC and T-cell) αvβ8 function in mice (**Fig. *S2***). B-line mice were the most robust line and were used as homozygous B-line *ITGB8* BAC;*itgb8*-/- mice (hereafter referred to as B-line) to conduct the majority of antibody efficacy

studies. The B- and C-lines had 2 completely integrated copies of the BAC *ITGB8* Tg, and the D-line a single copy. The B-line was used for dose response experiments (**Fig. 1*B* and Fig. *S4***) and the results with the highest dose were replicated in the C-line (**Fig. 1 *C-M***). Thus, the B- and C-lines responded similarly to Ad-IL-1β and the B-line was used exclusively for subsequent experiments (i.e. CS + poly(I:C) and Ova) since the B-line bred better than the C-line. Mice were used between 2-6 months of age.

Antibody engineering and affinity maturation of clone 37E1: Hybridomas were generated exactly as described (*10*). The protocol for affinity maturation has been published elsewhere (*10*). Briefly, a scFv yeast display library at the size of $2x10^7$ was created via error-prone PCR (GeneMorph® II Random Mutagenesis Kit, Strategene) using amplification of both 37E1 V_H and V_L genes using V_H forward primer MMGap5VHprimer10 pYD4 (5' GACTATGCAGCTAGCGGTGCCATGGCAGAAGTGCAGCTGKTGGAGWCTGG-3'), V_H reverse primer MMVH4pYD4Gap3' (5'-GTTGAGCCTCCGGACTTAAGGTCGACTGAGGAGACGGTGACTGAGGTTCC-3') and V_K forward primer MMVK7pYD4Gap5' (5'-GGAGAAGGTAGTAGTGGATCCGCGCGCCAAATTGTTCTCACCCAGTCTCC-3') with V_K reverse primer MMGap3Vkprimer 1 (5'-GGCTTACCTTCGAAGGGCCCGCCTGCGGCCGCTTTGATTTCCAGCTTGGTGCCTCC-3'). Diversity was increased by decreasing template concentration and reamplifying the first round mutagenic library with Taq polymerase using error prone conditions (5 mM Mg^{2+}, 0.2 mM Mn^{2+}). The mutagenic V_H and V_K libraries underwent splice-overlap extension PCR using Pfu polymerase and the library co-transformed with linearized pYD4 into *Saccharomyces Cerevisiae* (strain EBY100) by the lithium acetate method and displayed as scFv on the surface of yeast (*54*). This yeast displayed scFv library was sorted sequentially 6 times with decreasing concentration of soluble αvβ8-AP, and binding was detected with a non-overlapping monoclonal antibody directed against the αv integrin subunit (clone 8B8(*20*)) during the FACS sorting and analysis process. Twenty-four randomly selected best binders after the final sort were affinity compared and sequenced. Clone B5 was chosen to convert into full-length immunoglobulin. The full-length immunoglobulin B5 was produced from stable transformed CHO cell lines as chimeric human-mouse IgG1 and mouse IgG2a after subcloning the V-genes into two different mammalian cell expression vectors (*57*). Experiments in mice were conducted with B5 in the mouse IgG2a format.

Intratracheal injections: Mice were anesthetized with intraperitoneal (IP) injection of Avertin (250 mg/kg). Then Ad-hIL-1β or Ad-LacZ (2.5×10^8 pfu in 75μl sterile PBS) was instilled intratracheally with a needle (Popper® 24G-1' Straight 1.25mm ball) using the direct visualized instillation (DVI) technique (*58*).

Recombinant Adenovirus: The recombinant E1-E3 deleted type 5 adenovirus, either empty (Ad-C) or expressing human active IL-1β (Ad-IL-1β), has been described in detail elsewhere (*59*). The replication-deficient virus was commercially amplified and purified by cesium chloride gradient centrifugation and PD-10 Sephadex chromatography, plaque titered on 293 cells and checked for wild-type contamination (ViraQuest Inc., North Liberty, IA). Recombinant type 5 Adenoviral vectors expressing Cre-eGFP fusion protein, eGFP, or LacZ were obtained from the Gene Transfer Vector Core (University of Iowa, Iowa City, IA).

Measurement of airway response to acetylcholine. B-line female mice were anesthetized with ketamine (100 mg/kg of body weight) and xylazine (10 mg/kg) within 24 hr of the last CS exposure. A

tracheostomy was performed, and a tubing adaptor (20 gauge) was used to cannulate the trachea. The mice were attached to a rodent ventilator and pulmonary mechanics analyzer (FlexiVent; SCIREQ Inc, Canada) and ventilated at a tidal volume of 9 ml/kg, a frequency of 150 breaths/minute, and 2 cm H_2O positive end-expiratory pressure. Mice were paralyzed with pancuronium (0.1 mg/kg intraperitoneally). A 27-gauge needle was placed in the tail vein, and measurements of airway mechanics were made continuously using the forced oscillation technique. Mice were given increasing doses of acetylcholine (0.1, 0.3, 1, 3 and 9.6 μg/g of body weight) administered through the tail vein to generate a concentration-response curve. Airway resistance (RL) was calculated using Flexivent software and comparisons between groups were made after baseline normalization (*60*). The provocative challenge (pc200) was calculated using linear regression analysis.

Ovalbumin sensitization and challenge: Six- to 12 week-old sex-matched and littermate control B-line mice were sensitized with 50 μg Ovalbumin (Sigma) emulsified in 1 mg of aluminum potassium sulfate in a total volume of 200 μl in PBS on days 0, 4, and 7; Control animals received an equal volume of PBS/aluminum potassium sulfate IP on days 0, 4, and 7. Bronchoalveolar lavage (BAL) was performed and lung harvested 3 weeks after sensitization and used for ELISA. Intranasal challenge with ovalbumin (100 μg Ova/40 μl of PBS) or with PBS alone was given on days 21, 22, and 23 to lightly anesthetized mice (isoflurane inhalation). In some experiments, poly I:C (InVivogen) was delivered intranasally (50 μg).

Mouse organ harvests and bronchoalveolar lavage (BAL): For BAL, the trachea was cannulated and the lungs were lavaged 5 times using 0.8 ml of sterile PBS with 5mM EDTA. The recovery of the total lavage exceeded 90%. The fractions were centrifuged (600 *g* for 10 minutes), and the supernatant from the first fraction collected and kept at –80°C for ELISA assays or TGF-β bioassays, performed as described (*20*); the cell pellets from all fractions were pooled and resuspended in 1.0 ml sterile PBS and the total cell count was determined using a hemocytometer. Differential cell counts were performed using cytospin preparations (Cytospin 3; Thermo Shandon), which were prepared by centrifuging at 800 rpm for 6 min. Differential cell counts were made by counting 200 cells using standard morphological criteria. The heart was punctured and the lungs perfused with 10 ml sterile PBS containing 50 U of heparin per ml (Sigma-Aldrich). The right lung was isolated and divided into its lobes, placed in 20 ml of 10% formalin and shaken vigorously for 30 s to inflate. The left lung was divided into 5 portions, the left upper and the right lower portion used for DNA harvest, the middle frozen for protein analysis and the right upper and the left lower placed in RNA later (Applied Biosystems/Ambion, Austin,TX).

Airway morphometry and immunohistochemistry: Measurements of airway inflammation were estimated using Hematoxylin and Eosin (H&E) stained slides and wall fibrosis was assessed by the presence of thick collagen bundles stained by the trichrome method essentially as described by Hogg (*61*), which expresses wall thickness as a function of area of the airway wall/basement membrane length determined using image analysis software (Image J, v1.36b). Microtome sections from H&E or trichrome stained sections of paraffin embedded mouse lungs were digitally imaged at 200X magnification (QCapture v2.68.2, Surrey, BC, Canada). The slides were coded and an investigator (S.M.) blinded to the experimental groups acquired 5 digital images representing each lung lobe (and two images from the largest lobe) and the images coded and catalogued. Airway inflammation was defined as the inflammatory infiltrate extending from the airway basement membrane towards the lung parenchyma. Airway fibrosis was defined as thick collagen bundles (stained blue in trichrome stains) below the airway basement membrane. A minimum of 12 airways were examined per mouse. For pSMAD3 analysis, deparaffinized sections underwent antigen retrieval (120°C for 20 min, followed by 90°C for 10 min). Sections were stained with anti-pSMAD3 (1:30) overnight at 4°C and after extensive washing, detected using labeled polymer-HRP Anti-Mouse (K4007) and DAB (Dako, Carpinteria, CA). Sections

were blinded and photomicrographs randomly taken from airways. The number of airway epithelial cells stained nuclei were expressed as a fraction of basement membrane (BM) length sampled. Similarly, slides stained with Periodic acid–Schiff–diastase were blinded and photomicrographs taken. The number of airway epithelial cells with positively staining intracytoplasmic globules were counted and expressed as a fraction of BM length. Results were converted to a mucin staining index where 1 or 2 = ratios below or above the mean of all values, respectively.

ELISA assays: Adult lung fibroblasts from 5 different donors (repeated a minimum of two times/donor) were seeded in to 24-well culture dishes at a density of 100,000 cells/well in DMEM supplemented with 10% FCS and antibiotics. Prior to experimentation, cell media was changed to serum free DMEM, and blocking antibodies were administered at a final concentration of 270 nM. Cells were incubated in blocking antibodies for 6 hr before removal of media, replacement of blocking antibodies and induction with 1 ng/ml rIL-1β. Cells were incubated for a further 24 hours, after which media was removed and cells lysed in RIPA buffer. CCl20 secretion was assessed via ELISA for Human CCL20/MIP-3α (R&D systems, Minneapolis, MN). Human αvβ8 was detected by sandwich ELISA using the affinity-matured clone 42 of the domain specific antibody11E8 to the βI domain as the capture antibody and a Psi domain antibody (clone 6B9) as the second antibody.

Gel filtration of secreted integrins and Fab preparation: Recombinant integrin αVβ8 (containing a C-terminal clasp with a 10 a.a. flexible linker HPGGGSGGGS between αv-V_{992} and β8-R_{684}) was purchased from R&D systems (Minneapolis, MN), and unclasped truncated αvβ8 (at V_{996}) was purified from transfected HEK293 cells stably overexpressing truncated αvβ8 via affinity chromatography (*20*). B5 Fab fragments were generated by papain digestion (Pierce) of the IgG followed by separation using Mono S ion-exchange chromatography (GE Healthcare). The homogeneity and purity of all protein preparations were verified by SDS-PAGE stained with Coomassie blue; protein concentrations were measured by microbicinchoninic acid assay (Pierce). To prepare integrin-Fab complexes 25μg of recombinant αvβ8 was incubated in a 6-fold molar excess of Fab, and incubated at room temperature for 30 min. To prepare integrin-RGD complexes, 25μg of recombinant αvβ8 was incubated in 100 μM RGD peptide for 30 min at RT. Size exclusion chromatography was performed by injecting samples into a Superdex 200HR (10/300) column connected to an AKTA FPLC system at a flow rate of 0.5ml/min. Columns were pre-incubated in TBS (20mM Tris-HCL pH 7.5, 150 mM NaCl) and supplemented as appropriate with divalent cations (1mM Ca^{2+} and 1mM Mg^{2+}, or 0.4 mM Mn^{2+}).

Western blotting, ligand binding assays, adhesion assays, TFG-β activation assays: These assays were performed exactly as described with the following slight modifications (*10*, *20*, *55*). In Fig. 1*a*, background adhesion of wild-type 293 cells to LAP is subtracted from the binding shown. Adhesion assays were performed with saturating concentrations of antibodies (anti-β1 and β5 integrins) to block to other LAP binding integrins expressed by 293 cells. For adhesion assays and TGF-β activations assays, 20 μg/ml and 0.1 μg/ml B5 were used, respectively. For cell staining LAP competition assays with B5, values of mock-transfected cells were subtracted from the MFI (Fig. 7A). A modified αvβ8-TEV-AP-LAP binding assay was designed to distinguish a non- competitive vs. competitive mode of inhibition by B5. ELISA plates were coated with various concentrations of LAP, blocked with PBS with 5% BSA for 1 hr and then supernatant from αvβ8-TEV-AP expressing cells were allowed to bind for 2 hr at RT in the presence of no inhibitor, or varying concentrations of GRRGELATIH or GRRGDLATIH (Elim Biopharmaceuticals, Hayward, CA) or B5.

Construction of αv-integrin AP fusion constructs, βI glycan wedge mutants, mouse-human ITGB8 chimeras, and antibody epitope mapping: The construction of tr-αvβ8, β8-AP and β3-AP have been

described (*20, 62*). The β6-AP construct was made by PCR using the following primer pair (Forward 5'-GGTACCAAGCTTGAACGATGTCCTACCTGTGGTGACCCC-3'; Reverse 5'-TCCGGAAGATCTGTTTGGAGGCTTCGGACAATCTTTTTC-3'). The PCR product was cloned between Hind III and Bgl II of AP-tag. Then the C-terminal β6-AP fusion was cut out with BstEII and Xho I and cloned into β6 cloned into pcDNAI neo.

The αv-TEV-AP fusion was prepared by inserting a linker (Forward 5'- CCGGCGAGAAC CTCTACTTCCAAGGAT; Reverse 5'-GGCCTAGGAACCTTCATCTCCAAGAGC-3') into the BspE1 site of the αv-AP pcDM8 construct. This creates a linker starting at αv-W_{995} followed by SGENLYFQGSG I_1I_2 of SEAP.

The β8 glycan wedge mutant was created by splice overlap extension PCR using b8 pCDNA as a template using the following primers pairs: (
5' GAC AAC AAC ATT ACT GTC ATC TTT GCA G 3', 5' GTT TGG TCG ACA TAA TGC TGT TGT TCC 3'; and 5' CTG CAA AGA TGA CAG TAA TGT TGT TGT C 3', 5' GTT TGG TCG ACA TAA TGC TGT TGT TCC 3'. The spliced PCR products were cloned into b8 LXSN neo between the BglII and SalI sites.

M-H chimeras: Chimeric mouse-human *ITGB8* were generated using PCR with the following paired primers h PflM1 Forward 5'-CTGGGTCCAGAATGTGGATGGTGTGTTCAAGAG-3', m-hBglII Reverse 5'-CCAGAGATCTTTTGTCTGTGGACTGCTTTTTCAAACTC-3'; mBglII Forward 5'-AAAAAGATCTTTGGAAACATAGACACCCTTGAAGGAGG-3', m-h SalI Reverse 5'-TGTTTGGTCGACGCGATGCTGTTCCATGACAGCAC-3'; m-h Psi1 mut Forward 5'-CTCTCTTTATAATACCCACTGAGAATGAAATCAATACCCAGGTG-3', m BglII Reverse 5'-CCAAAGATCTTTTGGTTGGGGACTGCTTTTTCAAACTC-3'; m-h Psi1 WT forward 5'-CTCTCTTTATAACGTCAAGTGAGAATGAAATC-3', m BglII Reverse 5'-CCAAAGATCTTTTGGTTGGGGACTGCTTTTTCAAACTC-3'; m-h PflM1 Forward 5'-CTGGGTCCAGAATGTGGATGGTGTGTTCAAGAG-3', PshA1 Reverse human 5'-CCAAAACCAAGACGGAAGTCACGGGAAAAAAAGGCCATTTTTCTAGATAA ATCATTTCC-3'; h-BglII Forward: 5' CAGTTCATAGACAGAAGATCTCTGG 3', DraIII Reverse 5'-TTCTCATCACACTGT GG ACACTTGGAATCTAG-3'; h DraIII Forward 5'-TATATACACAGTGTGATGAGAATAAATGTCATTTTGATGAAGATCAG-3', h AleI Reverse 5'-TTCCACACACACGTGCC-3'; m-h Dra III Forward 5' -AAGTGTCCACAGTGTGATGACAGTAGATGTCATTTTGATGAAGATCAG-3', m-h HindIII Reverse 5'-TCCAAGCTTAGTTTTGTGACATAGACATTTCCCACAAATACAAACTCC-3'. The fine mapping of the B5 epitope was made with the following primers: Pair 1 (RLY) F: 5'-GGAAATGATTTATCTAGAAAAATGGCC-3', R: 5'-GGCCATTTTTCTAGATAAATCATTTCC-3'; Pair 2 (KFY): F: 5'-CTAAAAAAATGGCCTTTTATTCCCGTGAC-3', R: 5'-GTCACGGGAATAAAAGGCCATTTTTTTAG-3'; Pair 3 (KLF): F: 5'-CTAAAAAAATGGCCCTTTTTTCCCGTGAC-3', R: 5'-GTCACGGGAAAAAAGGGCCATTTTTTTAG-3'; Pair 4 (RLF): F: 5'-GATTTATCTAGAAAAATGGCCCTTTTTTCCCGTG; R: 5'-CACGGGAAAAAAGGGCCATTTTTCTAGATAAATC-3'; Pair 5 (RFY): F: 5'-GATTTATCTAGAAAAATGGCCTTTTATTCCCGTG, R: 5'-CACGGGAATAAAAGGCCATTTTTCTAGATAAATC-3'; Pair 6: (KFF): F: 5'-CTAAAAAAATGGCCTTTTTTTCCCGTGACTTC-3', R: 5'-GAAGTCACGGGAAAAAAAGGCCATTTTTTTAG-3'; Primer pair 7 (IGTSP): F: 5'-GAGGATTTTATTTCAGGTGG-3', R: 5'-CCACCTGAAATAAAATCCTC-3'; Primer pair 8 (VRTSP): F: 5'-GGTGGATCACGAAGTGAACGTTGT G-3', R: 5'-C ACAACGTTCACT TCGTGATCCACC-3'; Primer pair 9 (VGISP): F: 5'-CGTTGTGATATTGTTTCCAGTTTG-3', R: 5'-CAAACTGGAAACAATATCACAACG-3'; Primer pair 10 (VGTNP): F: 5'-GTTTCC

AATTTGATAAGCAAAGGC-3', R: 5'-GCCTTTGCTTATCAAATTGGAAAC-3'; Primer pair 11 (VGTSS): F: 5'-CAAAGGCTGTTCAGTTGATTCAATAG, R: 5'-CTATTGAATCAACTGAACA GCC TTT G-3'. All clones were sequenced and verified. Transfections or retroviral transduction of constructs were performed exactly as described (*20*).

Microarray: Primary cultures of human fetal tracheal fibroblasts (*N*=3) were treated 16 hour with control IgG (W6/32) neutralizing anti-β8 (37E1) or a pan-TGF-β isoform neutralizing antibody (1D11). For each hybridization, Cy3-labeled cRNA from a fetal tracheal fibroblast sample treated with isotype control IgG, anti-β8 (37E1) or anti-TGF-β (1D11) was hybridized together with equal amounts of Cy5-cRNA from a sample of same patient treated with a different antibody. Labeled cRNAs were hybridized to 70-mer oligonucleotide microarrays (Operon Human Genome 70-mer Oligo Set Version 2.0, Operon Bio-technologies, Huntsville, AL) representing 23044 probes of which 13509 were unique and annotated. Arrays were scanned using the Axon 400B scanner (Molecular Devices, Sunnyvale, CA) and median pixel intensities were extracted with Genepix software (Molecular Devices) (*59*).

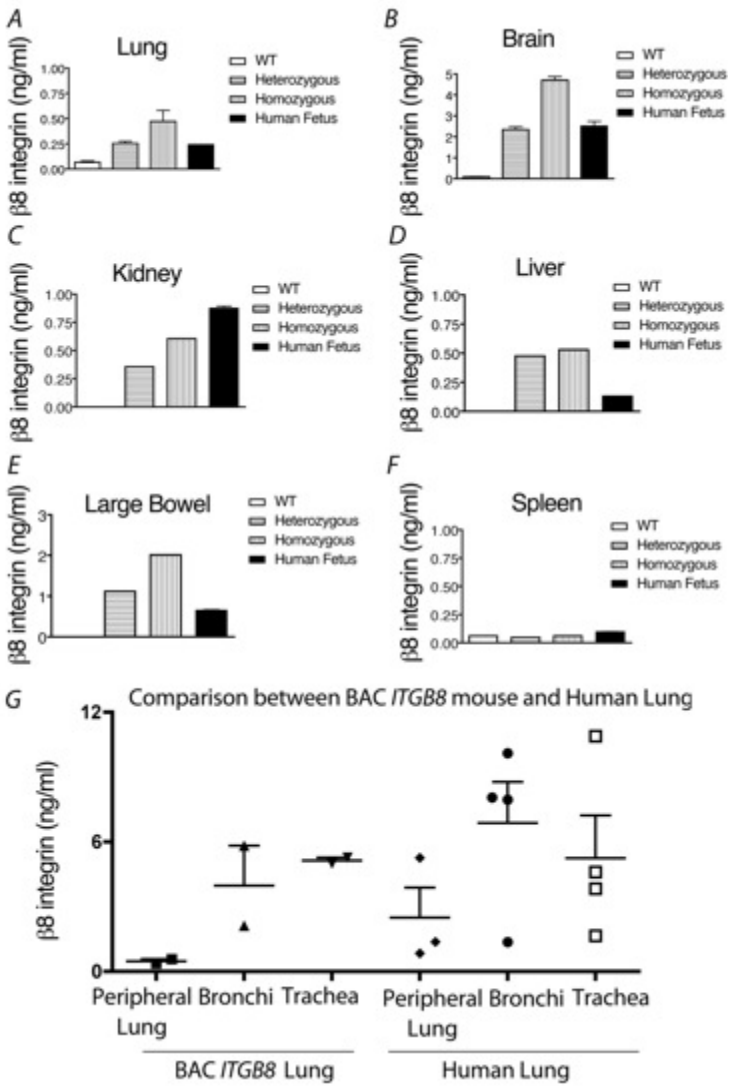

Fig. *S1*: *ITGB8* BAC Tg mice express αvβ8 at similar expression levels and tissue distribution to humans.

Expression of αvβ8 in lysates from adult B-line *ITGB8* BAC mouse organs or in human fetal organs (21 wks gestation) or adult human lung, as measured by sandwich ELISA. Shown are lung (***A***), brain (***B***), kidney (***C***), liver (***D***), large bowel (***E***) or spleen (***F***) from wild-type mice (WT) to demonstrate the background of the assay, and mice heterozygous or homozygous for the BAC *ITGB8* transgenic locus. *N*= at least 3 for the lung panel, at least 5 for the brain panel and at least 2 for all other organs. ***G***) To compare adult human lung to adult B-line *ITGB8* BAC mouse lungs, trachea, bronchi and peripheral lung from adult human lung and adult BAC mouse lung were microdissected, lysed and tested by ELISA. *N*=3 normal human lung samples from different donors; *N*=2 mouse BAC lung samples. Concentration is derived from a standard curve using recombinant human secreted αvβ8 (R&D Systems).

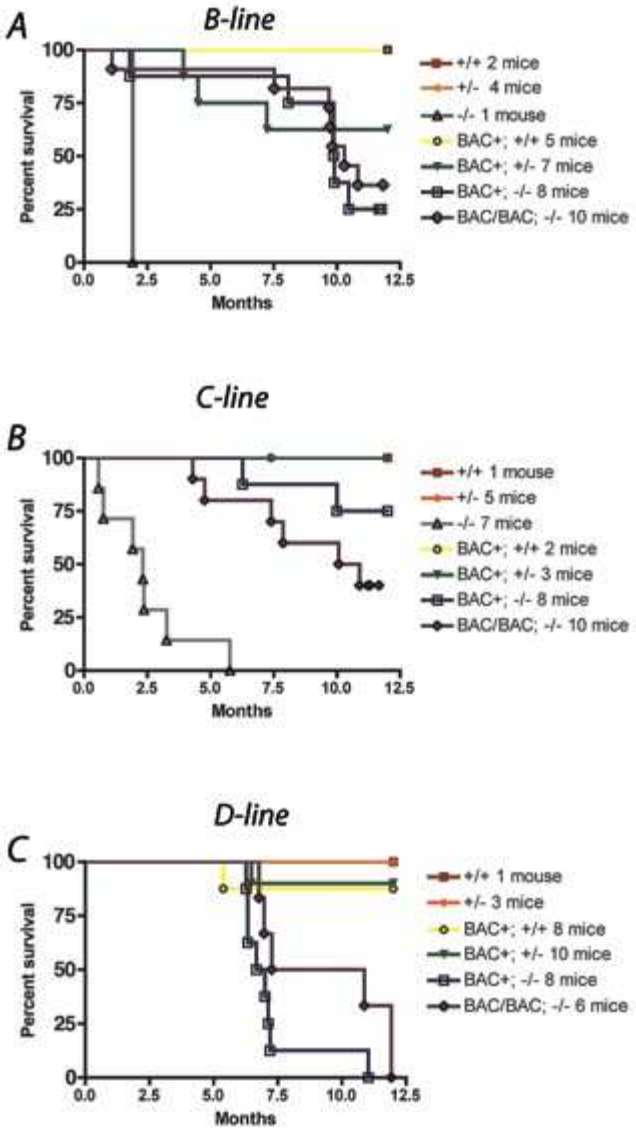

Fig. *S2*: *ITGB8* BAC transgene rescues early lethality of mouse *itgb8* deficiency. Four founders (designated lines A-D) expressing fully integrated copies of the BAC *ITGB8* transgene were identified by PCR with primers designed to the 5' and 3' BAC boundaries. Of these, 3 lines transmitted the BAC transgene to progeny and were designated lines B-D. Kaplan-Meier survival curves of mouse lines B-D (***A-C***) BAC Tg mice crossed to *itgb8* +/- mice. Mice are intercrosses between FVB/N and C57B/6 and the mixed progeny are all littermates. A few *itgb8* -/- mice survive to live birth, but most die early in gestation. Some of the older (>6mos) BAC *ITGB8*;*itgb8*-/- mice develop a scoliosis phenotype, which leads to poor mobility and feeding requiring euthanasia in accordance with IACUC guidelines. For the purposes of the survival statistics, the mice are considered dead the day of euthanasia.

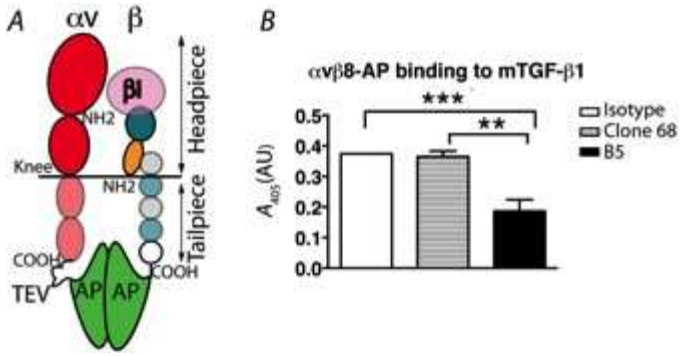

Fig. *S3*: Secreted human αvβ8 integrin–placental AP fusion proteins bind to murine latency-associated peptide. ***A***) Cartoon of the domain structure of the secreted **αvβ8** integrin with a flexible 11 a.a. linker (TEV) at the junction of the αv C-terminus and the N-terminus of secreted alkaline phosphatase (AP). The integrin splice sites at the junction of the extracellular and transmembrane domains are indicated (COOH). For secreted integrin binding assays, supernatant was quantified by AP activity assay, concentrated as appropriate and applied directly to ligand-coated 96-well plates. ***B***) Murine TGF-β1 from transfected P3U1 myeloma cells was captured using anti-LAP (clone TW4-16B4, 2 μg/ml) coated wells. After extensive washing secreted human αvβ8-TEV-AP was added to the wells and allowed to bind in the presence of control non-blocking antibodies (clone 68 or W6G2) or to B5 (all at 0.75 μg/ml). Shown is relative absorbance minus signal from BSA coated wells. *N*=4, ***p<0.001, **p<0.01 as determined by ANOVA and Tukey's post-test.

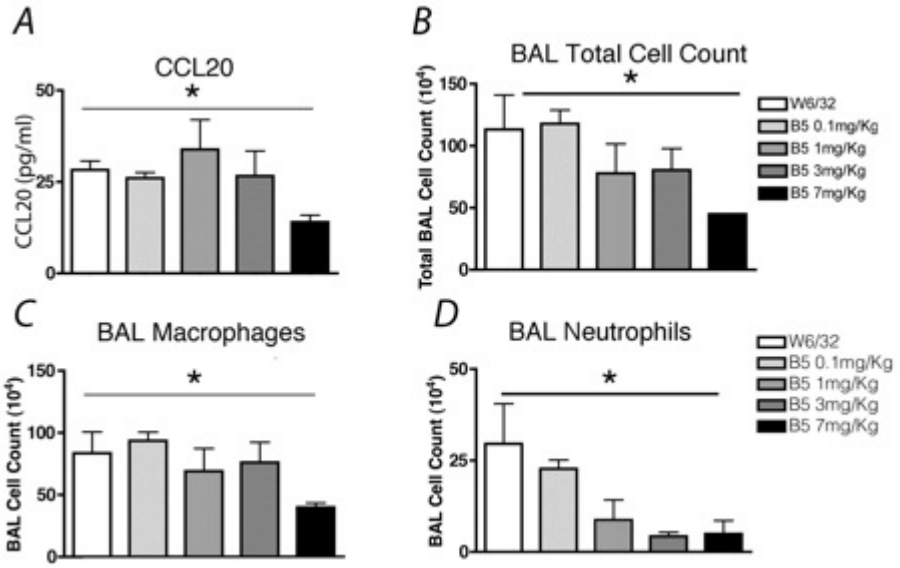

Fig. *S4*: Dose response of B5 antibody treatment of intratracheal-Ad-IL-1β injected B-line *ITGB8* BAC Tg mice.

Lung CCL20 (***A***), total BAL cell counts (***B***), BAL macrophages (***C***), and neutrophils (***D***) at varying doses of B5 compared with control IgG (W6/32) 14 days after IT-Ad-IL-1β. **P*<0.05 as determined by ANOVA and p-test for trend.

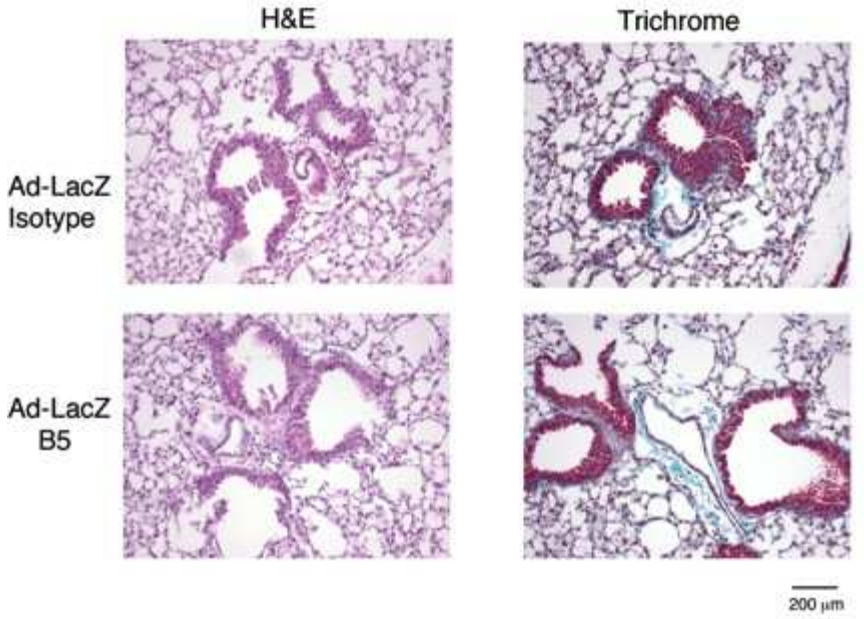

Fig. *S5*: Antibody treatment with B5 does not have any effect on lung morphology
Shown are the control groups for Fig. 1

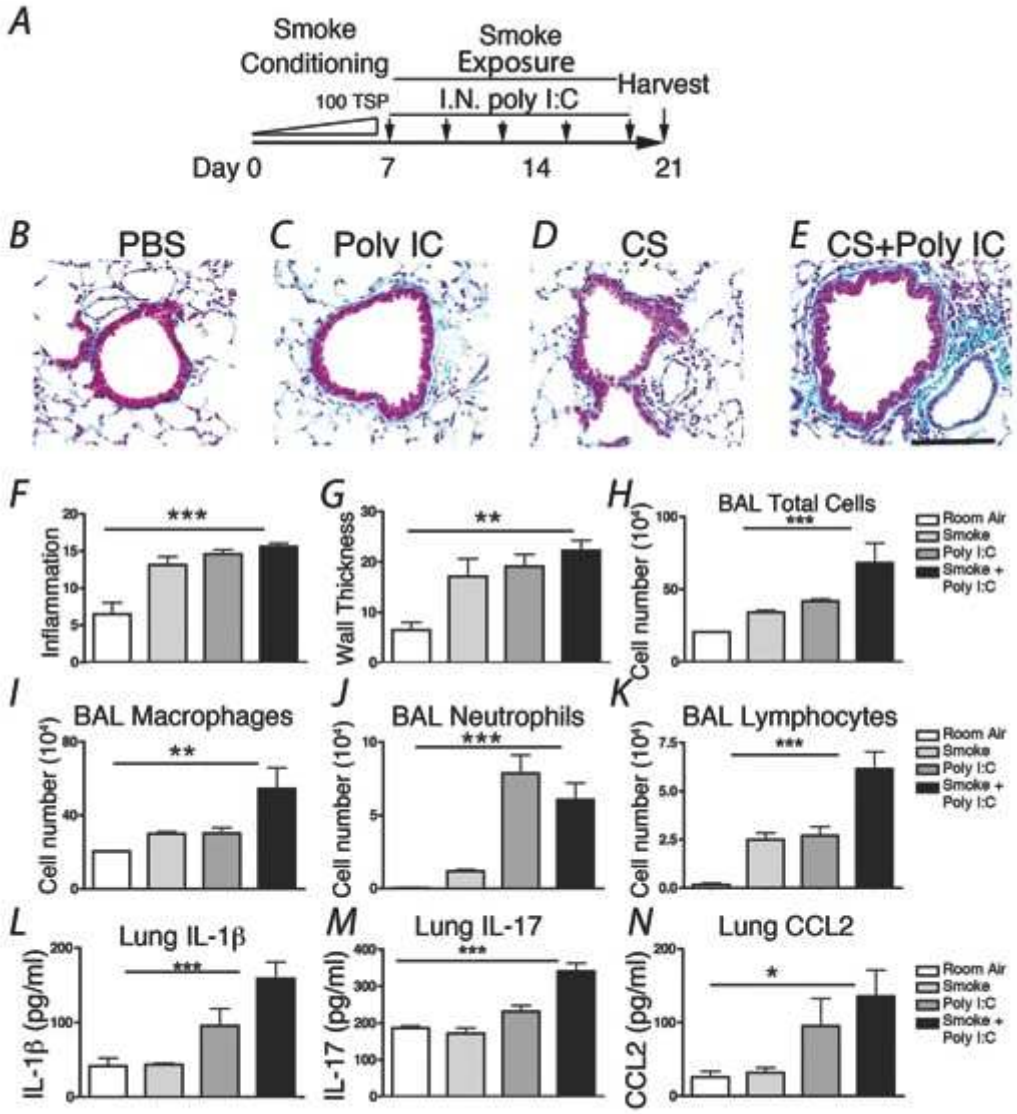

Fig. *S6*. Cigarette smoke and poly(I:C) synergistically produce airway disease that resembles COPD in humans.

A) Schematic of the 3 wk cigarette smoke dosing schedule. ***B-D***) Micrographs of trichrome stained section demonstrate that airway wall thickening only markedly occurs in mice treated with both cigarette smoke and poly(I:C). Comparisons of the effects of smoke alone, poly(I:C) alone and smoke and poly (I:C) combined on wall inflammation (***E***), wall thickness (Bar=100 μm) (***F***), BAL total cells (***G***), macrophages (***H***), neutrophils (***I***), lymphocytes (***J***), Lung IL-1β (***K***) lung IL-17 (***L***) and lung CCL2 (***M***) protein. **P*<0.05, ***P*<0.01, ****P*<0.001 as determined by ANOVA and Tukey's post-test.

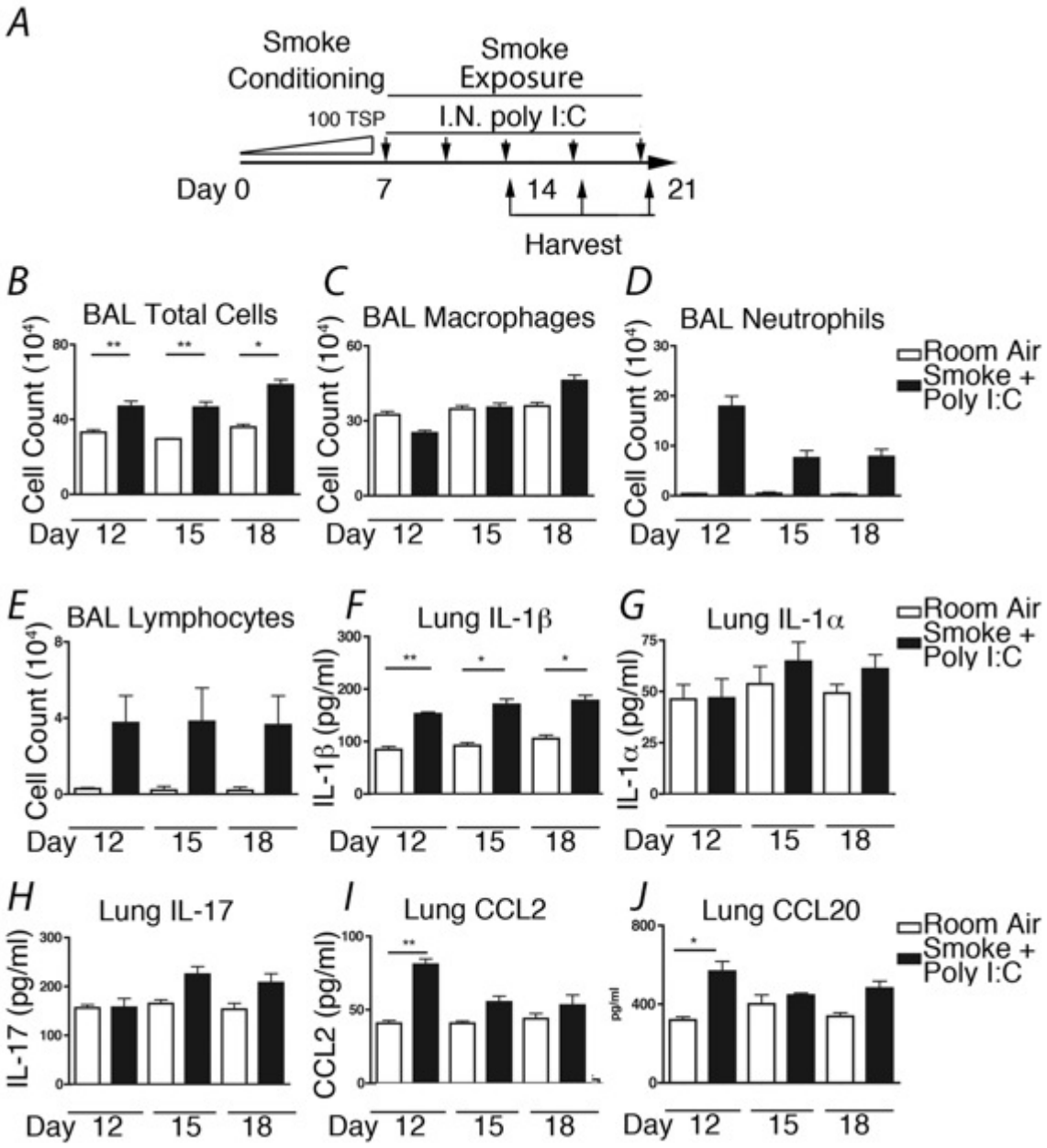

Fig. *S7*: Effects of combined exposure of cigarette smoke and poly(I:C) on inflammation and inflammatory mediators.

A) Treatment protocol and harvest time points. ***B-J***) Comparisons of the effects of room air vs. cigarette smoke and poly I:C combined on BAL total cells (***B***), macrophages (***C***), neutrophils (***D***), lymphocytes (***E***), Lung IL-1β (***F***), Lung IL-1α (***G***), lung IL-17 (***H***) and lung CCL2 (***I***) or lung CCL20 protein (***J***). *p<0.05, **p<0.01, ***p<0.001 as determined by ANOVA and Tukey's post-test.

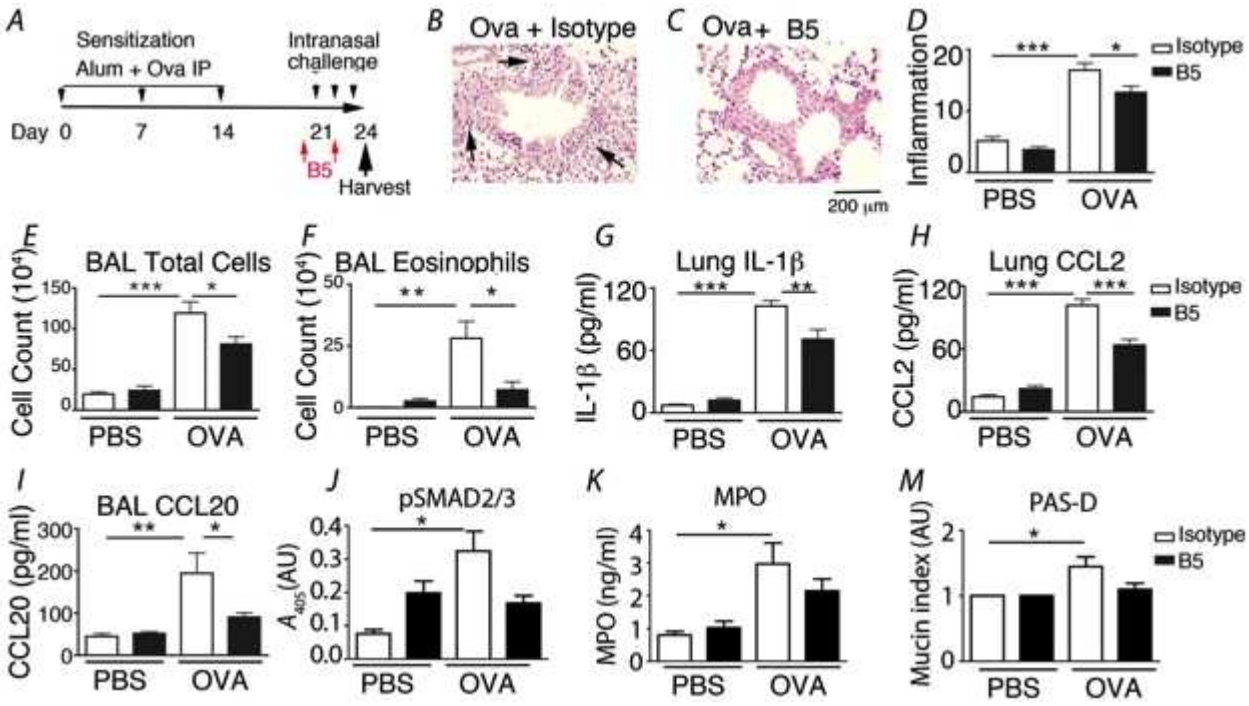

Fig. *S8*) B5 antibody treats allergic airway inflammation.

A) Schematic of protocol for ovalbumin (Ova) sensitization, challenge and B5 treatment. ***B***) Ova challenge induces airway inflammation (arrows), which is reduced by treatment with B5 (***C***). ***D)*** Airway inflammation determined by morphometry. ***E,F***) BAL total cell and eosinophil counts. ***G***) IL-1β, (***H***) CCL2, and CCL20 (***I***) are increased by Ova challenge and decreased by B5. ELISAs from lung homogenates (***G,H***) or BAL (***I***). Open bars = isotype control mice and filled bars, B5 treated mice. *N*=6, PBS + isotype, or PBS + B5; *N*=12, Ova + isotype, *N*=10, Ova + B5.**P*<0.05, ** *P* <0.01, *** *P*<0.001 by ANOVA and Tukey's post-test. *J*) pSMAD2/3; *K*) MPO; and *M*) Mucin staining are increased by Ova. There was a non-significant trend for a decrease by B5. *N*=4, PBS + isotype, or PBS + B5; *N*=5, Ova + isotype, *N*=5, Ova + B5.**P*<0.05.

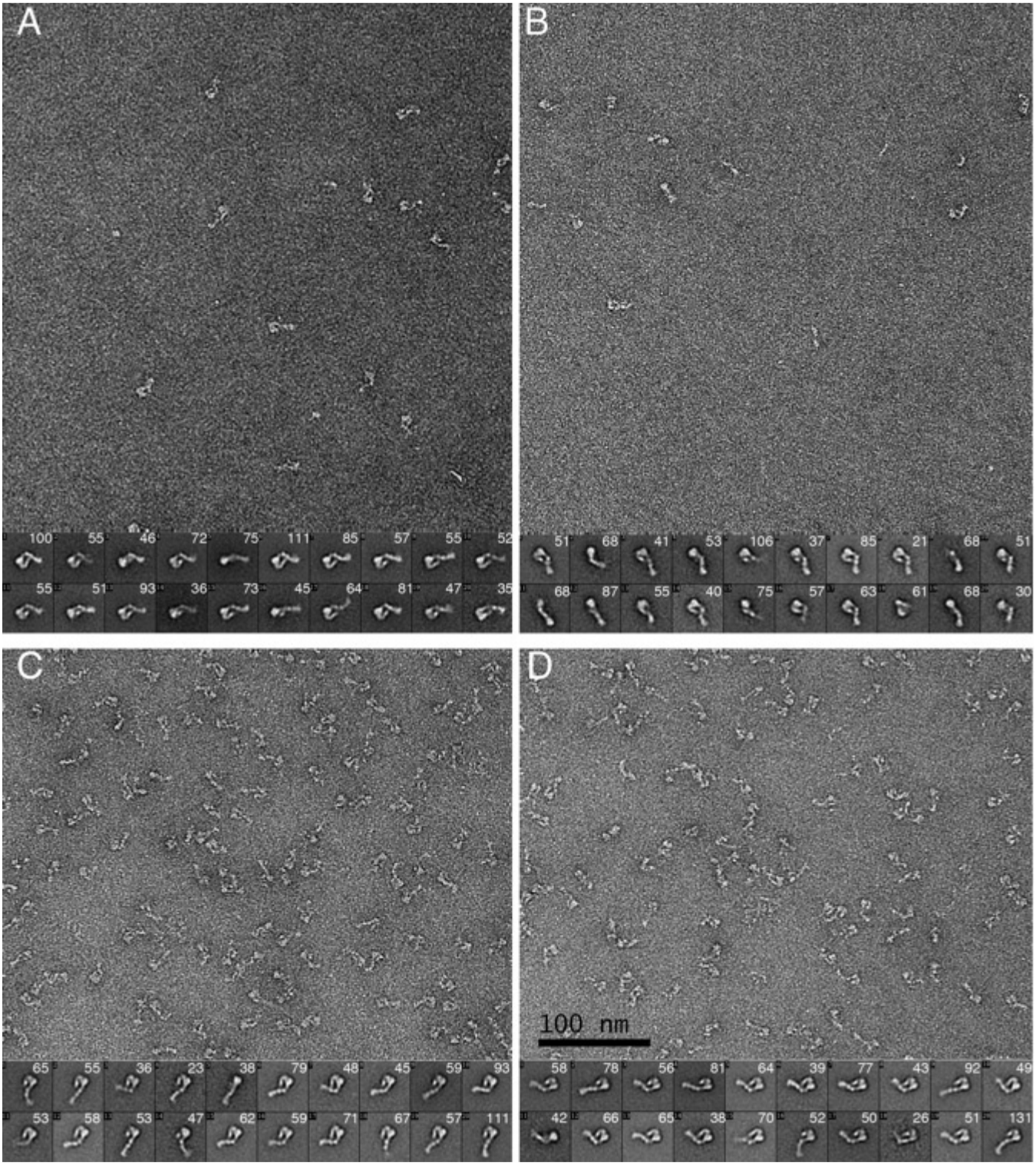

Fig. *S9*: Electron microscopy of integrin αvβ8.
Negative EM staining of clasped (***A***) and unclasped αvβ8 (***B-D***). In ***A-C*** buffer contained Ca^{2+} and Mg^{2+}. In ***D***, buffer contained Mn^{2+}. ***C, D***) Buffer included RGD peptide (GRRGDLATIH). Shown are raw images above the class averages. The numbers of particles seen in each of the class averages are shown. Scale: bar = 100 nM

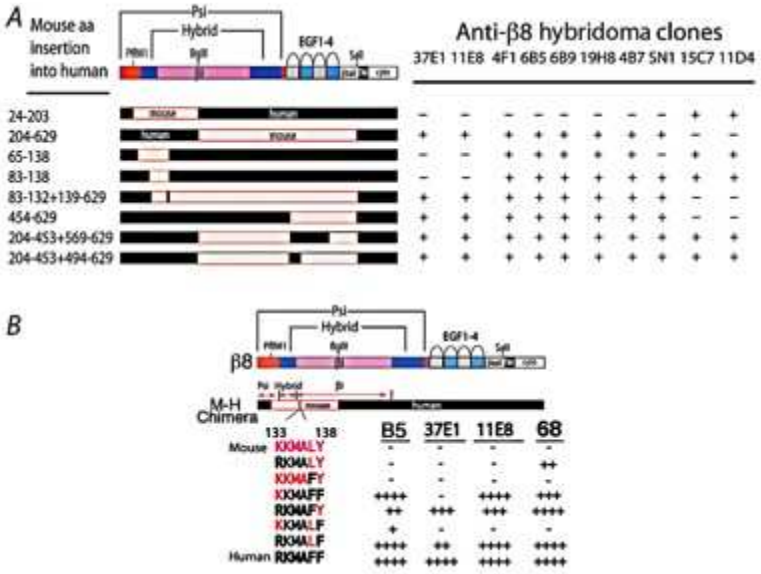

Fig. *S10*: β8 antibody epitope mapping.

A) Schematic of the chimeras consisting of integrin β8 sequences of mouse (white boxes) and human (black). Numbering corresponds to the mature human β8. Degree of binding affinity is indicated as binding (+) or no binding (-) to respective construct. ***B***) Fine mapping of the blocking antibody binding to the 133-138 epitope based on binding data to the 83-132+139-629 construct. Mouse sequence in red and human in black. Binding is relative to 11D4 MFI (Neg (-) =<29%; + =30-49%; ++ = 50-99%; +++ = 100-149%; ++++ = > 150%). Clone 68 is a derivative of 11E8. Experiments were conducted in triplicate.

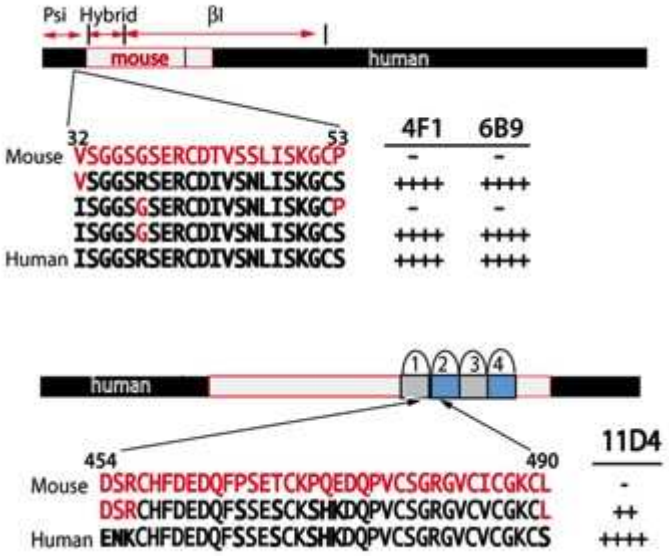

Fig. *S11*: Non–function-blocking antibodies binding to the Psi, hybrid, or epidermal growth factor (EGF) 1–2 domains.

Schematic of the chimeric β8 integrins used for epitope mapping. Degree of binding affinity of antibodies to psi domain (4F1 and 6B9) or anti-EGF 1-2 (11D4) is indicated as binding (+) or no

binding (-) to respective constructs. Mouse sequence in white boxes and human in black. Numbering corresponds to the mature human β8 protein. Mouse amino acids are in red and human in black.

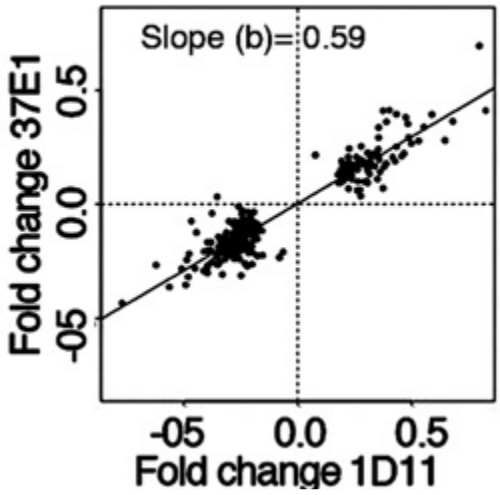

Fig. *S12*: Genome-wide comparison of the effects of β8 and TGF-β neutralizing antibodies on human fibroblast gene expression.
Plot of fold change (Log2) of differentially expressed genes by treatment with anti-β8 (37E1) or anti-TGF-β (1D11) vs. control antibody (W6/32). Each point represents one gene. Human fetal tracheal fibroblasts were used as a model of prosynthetic contractile fibroblasts (*19*). Fibroblasts were treated with neutralizing anti-integrin αvβ8, anti-pan-isoform TGF-β or isotype control antibody (*N*=3 different donor cell lines) all at 100 μg/ml for 24 hrs prior to harvest. Genes were deemed as differentially expressed when its B-statistic was greater than zero. Slope (b) indicates an effect size 59% of 37E1 compared with anti-pan TGF-β. ****P*<0.0001 by non-linear regression and F-test of EC_{50} values.

Clone	Framework 1	CDR1	Framework 2	CDR2	Framework 3	CDR3	Framework 4
V_H							
37E1wt	EVQLVESGGGLVQPGGSLNLSCAASGFVFS	RYWMS	WVRQAPGKGLEWIG	EINPDSSTINYTSSLKD	KFIISRDNAKNTLYLQMNKVRSEDTALYYCAC	LITTEDY	WGQGTSVTVSS
37E1B5	EVQLVESGGGLVQPGGSLNLSCAVSGFVFS	RYWMS	WVRQAPGKGLEWIG	EINPDSSTINYTSSLKD	KFIISRDNAKNTLYLQMNKVRSEDTALYYCAC	LITTEDY	WGQGTSVTVSS
V_L							
37E1wt	QIVLTQSPSSMYASLGERVTIPC	KASQDINSYLS	WFQQKPGKSPKTLIY	RANRLVD	GVPSRFSGSGSGQDYSLTISSLEYEDMGIYYC	LQYDEFPYT	FGGGTKLEIKA
37E1B5	QIVLTQSPSSMYASLGERVTIPC	KASQDINSYLS	WFQQKPGKSPKTLIY	YANRLVD	GVPSRFSGSGSGQDYSLTISSLEYEDMGIYYC	LQYDEFPYT	FGGGTKLEIKA

Fig. *S13:* V_H and V_L sequences of 37E1 and B5.
Amino acid sequences Complementary determining regions (CDRs) for each antibody. Highlighted in red boxes are differences between B5 and the parental antibody.

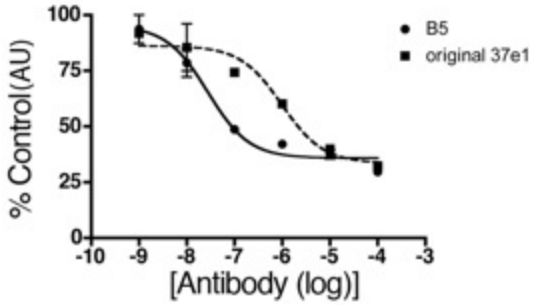

Fig. *S14*: B5 improves the ability of 37E1 to inhibit the binding of soluble αvβ8 to latency-associated peptide.
Binding curves of LAP and secreted αvβ8-AP fusion protein to various concentrations of affinity matured B5 or 37E1 (hybridoma clone) relative to the binding of an isotype control antibody (μg/ml) The EC_{50} of B5 was 27 ng/ml compared with 975 ng/ml for 37E1. Error bars are s.e.m.

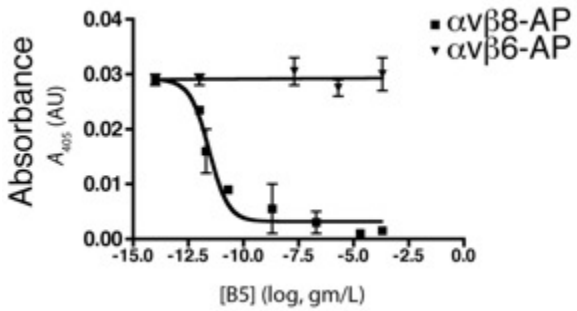

Fig. *S15*: B5 specifically blocks binding of αvβ8 and not αvβ6, to latency-associated peptide.
Binding of integrins measured calorimetrically. Secreted αvβ8-AP or αvβ6-AP incubated with immobilized LAP (10 mg/ml coating concentration) on 96 well plates in the presence of varying concentrations of B5 (log scale).

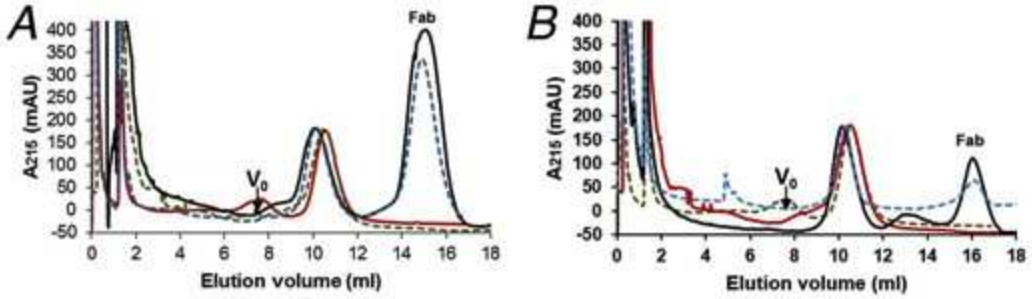

Fig. *S16*: Gel Filtration of clasped or unclasped αvβ8 in complex with B5 Fab.
Secreted αvβ8, either clasped or unclasped was allowed to bind to B5 Fab (***A***) or Clone 68 Fab (***B***) and SEC (Sephadex 200 10/300) performed. Shown is the elution profile of the clasped αvβ8 protein (black) or unclasped (blue) in 1 mM $Ca^{2+}/Mg^{2+}$with B5 Fab or Clone 68 Fab compared with the clasped αvβ8 (red) or unclasped (green) without Fab in 1 mM Ca^{2+}/Mg^{2+}. Void volume (V_0) and Fab are shown.

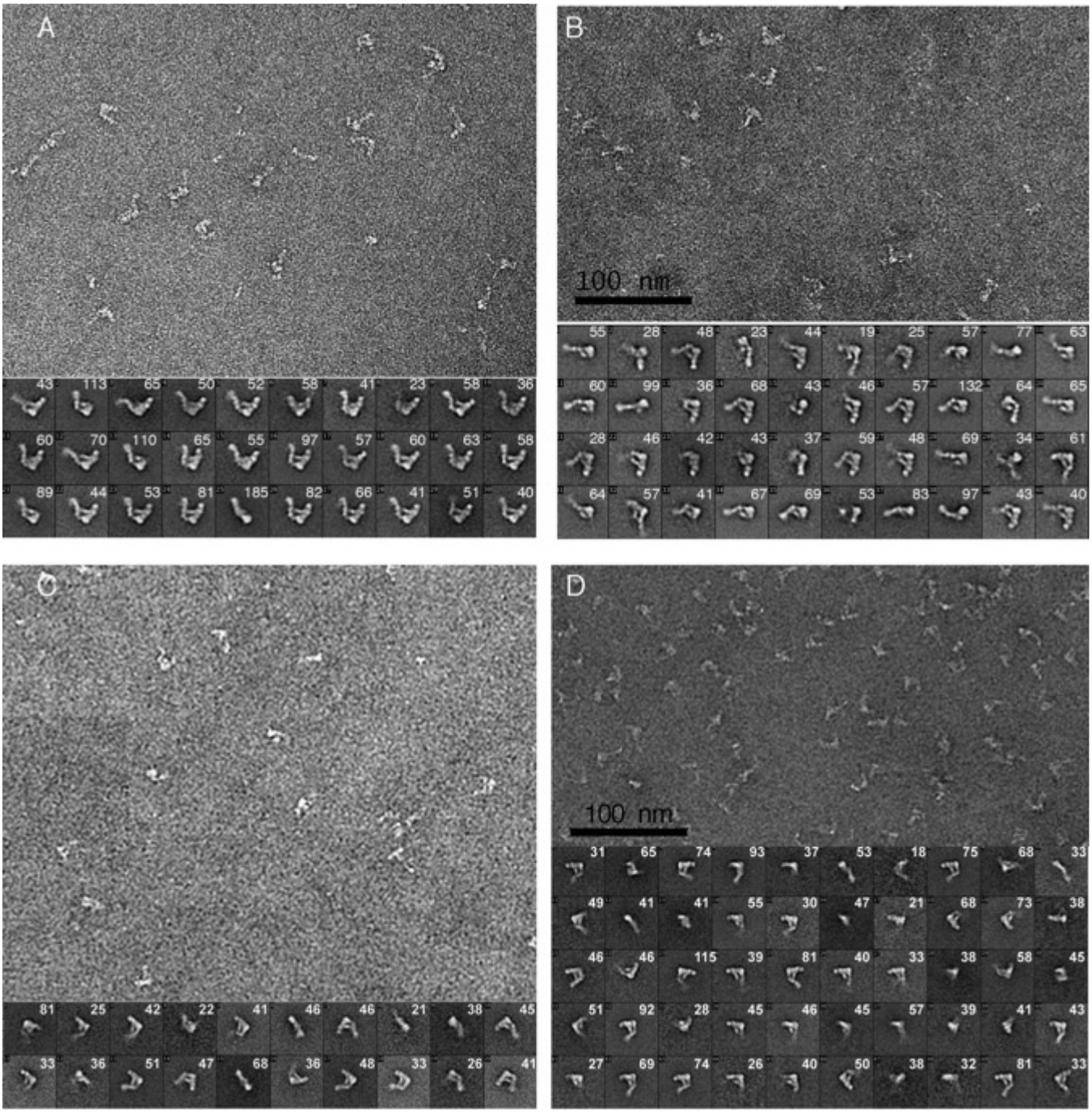

Fig. *S17*: Electron microscopy of integrin αvβ8.
Negative EM staining of clasped (***A,C***) and unclasped αvβ8 (***B,D***) in 1 mM Ca^{2+} and Mg^{2+} with B5 (*A,B*) or Clone 68 (*C,D*) Fab. Peak fractions were analyzed from the elution profile shown in **SFig. 6**. Shown are raw images above the class averages. The numbers of particles seen in each of the class averages are shown. The magnification of the raw images is the same. Scale: bar = 100 nM. The box width of the class averaged images on the top row is 35.4 nm and on the bottom 44.2 nm.

Table *S1*: Fibroblast differentially expressed gene array data. Comparison of anti-TGF-β (1D11) or anti-β8 (37E1) versus Isotype control

Gene Symbol[1]	Log2 Mean Signal Intensity	1D11 Log2 fold change	B>0 [2]	37E1 Log2 fold change	B>0
AADACL1	9.2	0.8	*	1.0	
ABI3BP	10.4	1.4	*	1.2	*
ACTA2	13.3	0.8	*	0.8	
AKR1B10	7.9	1.3	*	1.1	
ALDH1A3	11.5	1.2	*	1.1	
ALDH1B1	8.9	0.9	*	0.9	
ALS2CR4	10.5	0.9	*	0.9	
ANGPT1	11.5	0.8	*	0.9	
ANLN	10.1	0.9	*	0.9	
ARHGAP6	10.1	1.3	*	1.1	
ASNS	13.8	0.8	*	0.8	*
ASPM	10.0	0.8	*	0.9	
ASPM	8.7	0.8	*	0.9	
AURKA	10.9	0.8	*	0.9	*
AURKA	9.5	0.8	*	0.8	*
BDKRB2	12.2	1.3	*	1.3	*
BLM	7.8	0.9	*	0.9	
BMP5	8.3	1.2	*	1.0	
BRRN1	7.7	0.8	*	0.9	*
BTC	8.5	1.1	*	1.1	
BUB1	9.0	0.8	*	0.9	
BUB1B	8.9	0.8	*	0.9	
C10orf116	13.6	1.4	*	1.2	
C12orf5	9.2	0.8	*	0.9	
C18orf22	10.1	1.2	*	1.1	
C1orf135	7.3	0.9	*	0.9	
C3orf26	10.4	0.9	*	1.0	
C5orf13	11.4	0.8	*	0.9	
C6orf105	7.5	0.9	*	0.9	
C9orf26	8.5	1.3	*	1.3	*
CCBE1	11.2	0.8	*	0.9	
CCDC102B	8.3	1.3	*	1.0	
CCL2	12.0	0.7	*	1.0	
CCL7	8.3	0.8	*	1.0	
CCNA2	9.1	0.8	*	0.9	
CCNB1	11.2	0.8	*	0.9	
CDC2	10.6	0.8	*	0.9	
CDC20	10.2	0.9	*	0.9	
CDC45L	8.2	0.8	*	0.9	
CDC6	8.6	0.8	*	0.9	
CDCA1	9.4	0.8	*	0.9	
CDCA3	9.6	0.9	*	0.9	
CDCA8	9.2	0.8	*	1.0	
CDH11	14.3	0.8	*	0.9	
CDKN3	11.5	0.8	*	0.9	
CDO1	12.7	1.2	*	1.1	
CENPE	9.7	0.8	*	0.9	

CENPL	10.1	0.8	*	0.9	
CFD	10.3	1.1	*	1.1	*
CHAC2	8.2	0.8	*	0.9	
CHAF1A	9.2	0.9	*	0.9	
CHI3L2	11.4	1.4	*	1.3	*
CHL1	8.6	1.2	*	1.1	
CHRDL2	7.8	0.7	*	0.9	
CHURC1	9.9	1.2	*	1.1	
CKAP2	10.5	0.9	*	0.9	
CLCA2	10.0	1.5	*	1.3	*
CLEC3B	12.0	1.5	*	1.3	*
CLIC3	9.6	1.2	*	1.1	
COL21A1	10.1	1.3	*	1.1	
COL4A6	11.1	1.3	*	1.2	*
COMP	9.3	0.8	*	1.0	
CPA4	12.2	0.8	*	0.9	
CREB5	8.8	1.2	*	1.1	
CTGF	15.4	0.8	*	0.8	*
CTPS	9.4	0.8	*	0.9	
CXorf38	8.7	0.8	*	0.9	
CYP2C18	10.0	1.1	*	1.1	
CYR61	11.8	0.6	*	0.8	*
DDIT4L	13.1	1.3	*	1.2	*
DHRS3	12.4	0.9	*	0.9	
DIAPH3	8.5	0.8	*	0.9	
DKFZp762E1312	8.9	0.9	*	0.9	
DKK1	9.4	0.8	*	0.9	
DKKL1	10.5	0.8	*	0.9	*
DPP4	11.7	1.3	*	1.1	
DPT	10.8	1.3	*	1.1	
DSCR2	11.7	0.9	*	1.0	
DTL	8.9	0.8	*	0.9	
ECOP	10.2	0.8	*	0.9	*
ECT2	10.0	0.8	*	0.9	*
EIF3S1	11.9	1.1	*	1.1	
EMP1	13.5	0.9	*	0.9	*
ESM1	8.8	0.7	*	0.9	
FADS1	10.9	0.8	*	0.9	
FAM40B	7.6	0.8	*	1.0	
FAM83D	8.9	0.9	*	0.9	
FBLN5	11.0	0.8	*	0.9	*
FGF1	9.5	0.9	*	0.9	
FGF18	10.6	0.8	*	0.9	
FGL2	9.3	1.4	*	1.2	
FHOD3	8.8	0.8	*	0.9	
FJX1	9.9	0.8	*	0.9	
FKBP5	8.1	0.9	*	0.9	
FKSG14	9.0	0.8	*	0.9	
FLJ12505	8.2	1.2	*	1.1	
FLJ32130	8.8	1.2	*	1.1	
FST	12.5	0.8	*	0.8	*
GADD45B	10.2	0.8	*	0.9	

GALNTL4	8.4	0.8	*	0.9	
GARS	14.5	0.9	*	0.9	*
GAS6	10.4	0.8	*	0.8	*
GDF15	11.3	0.8	*	0.9	
GHR	10.4	1.2	*	1.1	
GINS2	9.5	0.8	*	0.9	
GMNN	10.4	0.9	*	1.0	
GOLGA1	9.6	1.2	*	1.2	
GSTA4	11.7	1.2	*	1.1	
GTF3A	13.0	0.9	*	0.9	
GTSE1	8.4	0.8	*	0.9	*
H2AFJ	8.8	1.1	*	1.1	
HAPLN1	11.6	0.8	*	0.8	*
HAVCR2	7.4	1.2	*	1.1	
HCAP-G	9.1	0.8	*	0.9	
HELLS	8.8	0.8	*	0.9	
HINT3	10.1	1.7	*	1.6	*
HIST1H1C	11.1	1.2	*	1.1	*
HIST1H4L	8.3	0.9	*	1.0	
HMMR	9.4	0.8	*	0.9	
HOP	9.4	1.3	*	1.1	
ID2B	13.6	1.2	*	1.1	
ID3	13.3	1.4	*	1.3	*
IGFBP6	14.4	1.2	*	1.1	
IGFBP7	13.2	0.9	*	0.9	
ITGA11	10.9	0.7	*	0.8	
ITGBL1	12.3	0.7	*	0.8	*
ITGBL1	10.7	0.7	*	0.8	*
ITGBL1	9.9	0.8	*	0.8	*
K-ALPHA-1	13.6	0.9	*	0.9	
K-ALPHA-1	13.0	0.8	*	0.9	
K-ALPHA-1	13.0	0.8	*	0.9	
K-ALPHA-1	12.9	0.8	*	0.9	
K-ALPHA-1	13.1	0.8	*	0.9	
K-ALPHA-1	13.5	0.8	*	0.9	
K-ALPHA-1	12.9	0.8	*	0.9	
K-ALPHA-1	13.7	0.8	*	0.9	
K-ALPHA-1	13.3	0.8	*	0.9	
K-ALPHA-1	13.2	0.8	*	0.9	
K-ALPHA-1	13.3	0.8	*	0.9	
K-ALPHA-1	15.0	0.8	*	0.9	
K-ALPHA-1	13.2	0.8	*	0.9	
K-ALPHA-1	13.2	0.8	*	0.9	*
K-ALPHA-1	13.4	0.8	*	0.9	*
K-ALPHA-1	13.8	0.8	*	0.9	*
K-ALPHA-1	13.3	0.8	*	0.9	*
KBTBD10	10.7	1.6	*	1.3	*
KCNK15	8.4	0.9	*	0.9	
KCTD12	12.8	1.6	*	1.2	
KIF22	8.8	0.8	*	0.9	
KIF23	9.2	0.8	*	0.9	
KLHL6	8.3	0.9	*	0.9	

KNTC2	10.6	0.8	*	0.9	*
KPNA2	13.2	0.8	*	0.9	
KRT19	11.0	1.2	*	1.1	
KSP37	9.3	1.3	*	1.1	
LBH	10.7	0.8	*	0.8	*
LOC134147	12.6	1.2	*	1.1	
LOC148898	8.4	1.2	*	1.1	
LOC56902	10.2	0.9	*	0.9	
LPHN2	11.4	1.2	*	1.2	*
LRRFIP1	11.4	0.9	*	0.9	
LRRN3	9.9	1.2	*	1.1	
LTBP2	12.4	0.7	*	0.8	
LTBP2	10.6	0.7	*	0.8	
MAD2L1	10.2	0.8	*	0.9	
MAFB	10.0	1.2	*	1.2	*
MARS	12.3	0.9	*	0.9	*
MCM2	9.7	0.8	*	0.9	
MEGF6	8.4	0.9	*	0.9	
MELK	8.8	0.8	*	0.9	
METRN	11.3	1.2	*	1.1	
MFAP5	12.6	0.9	*	0.9	
MLF1IP	10.2	0.8	*	0.9	*
MMP1	11.9	0.6	*	0.7	*
MMP7	8.4	0.8	*	0.8	*
MTA2	11.1	0.9	*	0.9	
MTHFD2	12.6	0.8	*	0.8	
MX2	10.7	0.8	*	0.9	
MYO1D	12.1	0.8	*	0.9	
NAPE-PLD	10.1	1.1	*	1.1	
NHN1	10.6	0.7	*	0.8	*
NME1	12.8	0.9	*	0.9	
NOX4	7.0	0.8	*	0.9	
NR4A2	8.3	1.3	*	1.3	*
NR4A3	9.7	1.3	*	1.3	*
NTN4	10.2	0.8	*	0.9	
NULL	9.0	0.8	*	0.9	
NULL	12.2	1.1	*	1.1	
NULL	13.0	1.2	*	1.2	*
ODC1	11.6	0.9	*	0.9	
PBK	10.0	0.8	*	0.9	
PCOLCE2	12.5	1.2	*	1.2	*
PEG10	11.1	1.4	*	1.2	*
PLK2	10.9	0.8	*	0.9	
PLN	9.9	0.7	*	0.8	*
POSTN	14.8	0.8	*	0.8	
PPAP2A	11.9	1.2	*	1.0	
PPARG	9.5	1.2	*	1.1	
PPIL1	10.6	0.8	*	0.9	
PPIL5	9.0	0.9	*	0.9	
PPP1R1B	10.9	1.2	*	1.2	
PPP1R3C	11.7	0.9	*	0.8	*
PRC1	10.2	0.8	*	0.9	*

PRRT2	10.2	1.3	*	1.2	*
PTK9	13.3	0.9	*	0.9	
PTX3	12.7	0.8	*	0.9	
RAB13	14.0	1.1	*	1.1	
RAB3IP	7.5	0.8	*	0.9	
RAD51AP1	8.3	0.8	*	0.9	
RAMP2	8.5	1.2	*	1.1	
RASA4	9.8	1.2	*	1.1	
RBBP8	10.3	0.8	*	0.9	
RFWD3	9.0	0.8	*	0.9	
RIS1	12.3	0.9	*	0.9	
RNASE4	11.8	1.1	*	1.1	
RP11-11C5.2	10.7	0.8	*	0.9	
RPS6KA5	9.2	1.3	*	1.2	
SART2	11.9	0.9	*	0.9	
SAT	13.1	1.2	*	1.2	*
SCD	11.5	0.8	*	0.9	
SEMA3C	13.7	0.8	*	0.9	
SEMA5A	11.2	0.9	*	0.9	
SEPP1	14.6	1.2	*	1.1	
SERAC1	10.6	0.8	*	0.9	
SERPINA3	11.1	0.8	*	0.9	
SERPINE1	10.5	0.7	*	0.8	*
SERPINI1	10.7	1.4	*	1.2	*
SESN3	12.6	1.2	*	1.1	
SFRP2	11.0	1.2	*	1.1	
SGK	10.8	0.8	*	0.9	*
SHCBP1	9.9	0.8	*	0.9	
SIN3B	12.6	1.2	*	1.1	
SLC14A1	12.5	0.9	*	0.9	*
SLC1A4	10.0	0.8	*	0.9	
SLC25A4	12.0	0.9	*	0.9	
SLC27A3	11.4	1.2	*	1.1	
SLC2A6	9.0	0.9	*	1.0	
SLC7A5	10.1	0.8	*	0.9	
SLPI	12.6	0.8	*	1.0	
SMURF2	10.2	0.9	*	0.9	
SNAI2	12.8	1.3	*	1.2	
SNED1	11.0	1.4	*	1.3	*
SOCS2	9.7	1.2	*	1.1	
SPARCL1	8.4	1.2	*	1.0	
SPCS3	11.1	0.9	*	1.0	
SPOCK1	12.4	0.8	*	0.9	*
SRPX	13.2	1.2	*	1.0	
SSR3	12.8	0.8	*	0.9	
STMN3	12.9	1.2	*	1.1	
SULF1	12.5	0.8	*	0.9	
SYTL2	10.8	1.2	*	1.1	
TACC3	8.0	0.9	*	0.9	
TAGLN	14.5	0.8	*	0.8	*
TDO2	10.0	1.8	*	1.3	*
TGFB2	8.3	1.3	*	1.1	

TGFB2	10.4	1.4	*	1.2	*
TGFBR1	11.6	0.9	*	0.9	
TIMELESS	8.9	0.8	*	0.9	
TIMP4	9.2	1.2	*	1.1	
TLR5	8.5	1.1	*	1.1	
TM4SF20	7.6	0.8	*	0.9	
TMPO	8.9	0.9	*	0.9	
TNFAIP6	11.5	0.8	*	1.0	
TPM1	9.5	0.9	*	0.9	
TRIB3	11.9	0.8	*	0.8	
TRIP13	9.3	0.9	*	0.9	
TTK	9.1	0.8	*	0.9	
TUBB6	13.3	0.8	*	0.9	
TXNRD1	13.2	0.8	*	0.9	
UBE2C	10.9	0.8	*	0.9	
UBE2T	9.8	0.8	*	0.9	
UGCG	11.5	0.8	*	0.8	*
UHRF1	8.7	0.8	*	0.9	
VIL2	10.5	0.9	*	0.9	
VLDLR	9.6	0.9	*	1.0	
WBP1	12.6	1.2	*	1.1	
WDSOF1	12.3	0.9	*	0.9	

[1]represents 252 individual genes
[2] *=B>0

Table *S2*. Autrocrine TGF-β activation mediated by αvβ8 by human fetal tracheal fibroblasts.

Ontogeny	Best GOs	GO term	Genes	Count	Total	P-Value
	(Max: 30)			57	33972	
	Go Accession					
Cellular Component						
	GO:0044421	extracellular region part	ccl2 col4a6 hapln1 dkkl1 chi3l2 fbln5 dpt fgf18 mmp1 fjx1 cxcl2 bmp5 fgl2 chl1 spock1 fgf1 ugcg comp mmp7 ccl7 ctgf gdf15 igfbp6	23	910	2.19E-10
	GO:0005615	extracellular space	ccl2 dkkl1 chi3l2 fgf18 fjx1 mmp1 cxcl2 bmp5 fgl2 spock1 fgf1 ugcg mmp7 ctgf ccl7 gdf15 igfbp6	17	528	3.63E-09
Molecular function						
	GO:0005515	protein binding	fbln5 ctps clic3 fgf18 gadd45b blm angpt1 fgl2 creb5 nr4a2 gas6 fads1 ccnb1 fgf1 c5orf13 fhod3 fkbp5 cdc45l comp anln gdf15 dkk1 cdc2 ccl2 ghr dpt pln tagln mafb cdca8 diaph3 btc ect2 hist1h1c serpine1 prc1 cdc6 chaf1a aurka cxcl2 sgk cdkn3 tgfb2 chl1 dtl cdc20 gars cenpe ctgf ccl7 gmnn itga11 cdh11 igfbp6 cyr61 igfbp7 cebpg arhgap6 col4a6 id3 fst gins2 mars bmp5 ccna2 kbtbd10 aspm bub1b esm1 acta2 pcolce2	71	9005	2.44E-09
Biologic Process						
	GO:0048856	anatomical structure development	fgf18 blm angpt1 tgfb2 chl1 nr4a2 gas6 spock1 fgf1 ugcg serpini1 comp ctgf itga11 cdh11 clec3b dkk1 igfbp6 cyr61 cebpg igfbp7 ccl2 ghr dkkl1 emp1 id3 pln tagln fst mafb chrdl2 bmp5 aldh1a3 esm1 serpine1	35	2005	9.76E-19
	GO:0048731	system development	ccl2 ghr emp1 id3 pln fgf18 tagln blm mafb fst angpt1 tgfb2 chrdl2 bmp5 chl1 nr4a2 spock1 fgf1 aldh1a3 ugcg serpini1 comp ctgf clec3b cdh11 itga11 serpine1 cebpg	28	1605	1.26E-14
	GO:0032502	developmental process	fgf18 gadd45b blm sgk angpt1 tgfb2 chl1 nr4a2 gas6 fads1 spock1 fgf1 ugcg serpini1 comp ctgf clec3b cdh11 itga11 dkk1 igfbp6 cyr61 cdc2 cebpg igfbp7 ccl2 churc1 ghr ckap2 dkkl1 pln emp1 id3 tagln mafb fst chrdl2 bmp5 hells bub1b aldh1a3 esm1 serpine1	43	3347	3.12E-14
	GO:0000278	mitotic cell cycle	prc1 cdc6 aurka gtse1 bub1 cdkn3 hells ccna2 aspm cdca3 cdca8 ccnb1 bub1b cdc20 cenpe anln cdc2	17	326	7.12E-12
	GO:0007275	multicellular organismal development	fgf18 gadd45b blm angpt1 tgfb2 chl1 nr4a2 spock1 fgf1 ugcg serpini1 comp ctgf itga11 cdh11 clec3b dkk1 cebpg ccl2 churc1 ghr emp1 id3 pln tagln mafb fst chrdl2 bmp5 hells aldh1a3 serpine1	32	2299	8.33E-12
	GO:0007067	mitosis	aspm cdca3 cdca8 ccnb1 bub1b cdc20 cdc6 aurka gtse1 bub1 cenpe anln hells ccna2 cdc2	15	239	1.16E-11
	GO:0000087	M phase of mitotic cell cycle	aspm cdca3 cdca8 ccnb1 bub1b cdc20 cdc6 aurka gtse1 bub1 cenpe anln hells ccna2 cdc2	15	245	1.25E-11
	GO:0051301	cell division	aspm cdca3 cdca8 prc1 ccnb1 bub1b cdc20 cdc6 bub1 cenpe anln tgfb2 hells ccna2 cdc2	15	245	1.25E-11
	GO:0022402	cell cycle process	prc1 cdc6 aurka gtse1 bub1 cdkn3 tgfb2 hells ccna2 aspm cdca3 cdca8 ccnb1 bub1b cdc20 cenpe cdc45l anln	20	625	1.33E-10

		gmnn cdc2			
GO:0032501	multicellular organismal process	fgf18 gadd45b blm angpt1 tgfb2 chl1 nr4a2 spock1 cfd fgf1 ugcg serpini1 comp ctgf clec3b itga11 cdh11 dkk1 cebpg ccl2 churc1 ghr emp1 id3 pln mmp1 tagln fst mafb chrdl2 hells bmp5 kbtbd10 akr1b10 dhrs3 aldh1a3 tdo2 gpr176 mmp7 id2b bdkrb2 serpine1	42	3822	1.84E-10
GO:0000279	M phase	aspm cdca3 cdca8 ccnb1 bub1b cdc20 cdc6 aurka gtse1 bub1 cenpe anln hells ccna2 cdc2	15	306	2.19E-10
GO:0022403	cell cycle phase	aspm cdca3 cdca8 ccnb1 bub1b cdc20 cdc6 aurka gtse1 bub1 cenpe anln cdkn3 hells ccna2 cdc2	16	369	2.20E-10
GO:0007049	cell cycle	prc1 ckap2 cdc6 chaf1a aurka gtse1 bub1 cdkn3 tgfb2 hells ccna2 aspm cdca3 cdca8 ccnb1 cdc20 bub1b cenpe cdc45l anln gmnn cdc2	22	839	2.91E-10
GO:0048513	organ development	ccl2 ghr emp1 id3 pln fgf18 tagln blm mafb fst angpt1 tgfb2 chrdl2 bmp5 fgf1 ugcg aldh1a3 comp ctgf clec3b cdh11 itga11 serpine1 cebpg	24	1141	2.44E-09
GO:0005819	spindle	prc1 bub1b cdc20 cdc6 aurka cdc2 bub1 cenpe	8	78	6.83E-08
GO:0009653	anatomical structure morphogenesis	ccl2 dkkl1 emp1 id3 fgf18 angpt1 mafb tgfb2 chl1 gas6 fgf1 aldh1a3 esm1 comp ctgf dkk1 serpine1 igfbp6 cyr61 cebpg igfbp7	21	1047	9.11E-08
GO:0000775	chromosome, centromeric region	cdca8 mlf1ip bub1b cenpl hells bub1 cenpe	7	76	1.51E-06
GO:0051052	regulation of DNA metabolic process	cdc45l blm gmnn cdc6 cebpg id3	6	49	2.60E-06
GO:0008283	cell proliferation	gas6 spock1 btc bub1b cdc6 fgf1 emp1 bub1 fgf18 blm cdkn3 tgfb2 hells igfbp6 cyr61 igfbp7	16	745	3.02E-06
GO:0048869	cellular developmental process	ccl2 ckap2 emp1 id3 fgf18 gadd45b blm sgk angpt1 mafb tgfb2 chrdl2 bmp5 chl1 nr4a2 fads1 fgf1 bub1b aldh1a3 ctgf cdc2 cebpg	22	1810	3.02E-06
GO:0030154	cell differentiation	ccl2 ckap2 emp1 id3 fgf18 gadd45b blm sgk angpt1 mafb tgfb2 chrdl2 bmp5 chl1 nr4a2 fads1 fgf1 bub1b aldh1a3 ctgf cdc2 cebpg	22	1810	3.02E-06
GO:0000075	cell cycle checkpoint	cdc45l bub1b cdc6 ccna2 gtse1 bub1	6	56	4.84E-06
GO:0006950	response to stress	ccl2 chaf1a gtse1 id3 gadd45b blm sgk cxcl2 tgfb2 ccna2 dtl fads1 cfd cdo1 ccl7 gsta4 ctgf bdkrb2 serpine1 cebpg	20	1222	4.84E-06
GO:0001501	skeletal system development	ghr fgf18 comp ctgf tgfb2 chrdl2 cdh11 clec3b bmp5	9	209	8.35E-06
GO:0000074	regulation of cell cycle	bub1b cdc6 gtse1 bub1 cdc45l cdkn3 anln gmnn tgfb2 ccna2 cdc2	11	353	8.99E-06
GO:0051726	regulation of cell cycle	bub1b cdc6 gtse1 bub1 cdc45l cdkn3 anln gmnn tgfb2 ccna2 cdc2	11	359	1.03E-05
GO:0009887	organ morphogenesis	ccl2 fgf1 aldh1a3 fgf18 comp ctgf mafb angpt1 tgfb2 serpine1 cebpg	11	362	1.08E-05